Available online at www.sciencedirect.com

ScienceDirect

Journal of Hydro-environment Research 9 (2015) 268–280

Journal of Hydro-environment Research

www.elsevier.com/locate/jher

A hydraulic roughness model for submerged flexible vegetation with uncertainty estimation

A.O. Busari [a], C.W. Li [b,*]

[a] Department of Civil and Environmental Engineering, The Hong Kong Polytechnic University, Hong Kong, China
[b] Dept. of Civil and Environmental Engineering, The Hong Kong Polytechnic University, Hong Kong, China

Available online 17 December 2014

Abstract

Submerged vegetation is a key component in natural and restored rivers. It preserves the ecological balance yet has an impact on the flow carrying capacity of a river. The hydraulic resistance produced by submerged flexible vegetation depends on many factors, including the vegetation stem size, height, number density and flow depth. In the present work a numerical model is used to generate synthetic velocity profile data for hydraulic roughness determination. In the model turbulence is simulated by the Spalart-Allmaras closure with a modified length scale which is dependent on the vegetation density and vegetation height to water depth ratio. Flexibility of vegetation is accounted for by using a large deflection analysis. The model has been verified against available experiments. Based on the synthetic data an inducing equation is derived, which relates the Manning roughness coefficient to the vegetation parameters, flow depth and a zero-plane displacement parameter. Furthermore, the uncertainty of the inducing equations in the estimation of the Manning roughness is assessed and the propagation of the uncertainty due to the variability of the vegetation and flow parameters existed in nature is investigated by using the method of Unscented Transformation (UT). The UT is found efficient and gives a more accurate estimation of the mean Manning roughness coefficient and provides information on the covariance of the roughness coefficient.

Keywords: Flexible vegetation; Hydraulic roughness; Inducing equation; Unscented transformation; Zero-plane displacement

1. Introduction

Submerged vegetation is a key component in natural and restored rivers. The ongoing promotion of the natural development of wetlands and other restoration projects to enhance development within river basins favors the growth of submerged vegetation. Vegetation preservation is of great significance to the ecological balance yet has a hydraulic impact on the flow carrying capacity. The hydraulic resistance produced by submerged flexible vegetation depends on many factors, including the vegetation stem size, plant height, number density and flow depth.

Carollo et al. (2005) reported that the application of the well-known Kouwen's method overestimated the flow resistance in an open channel with flexible vegetation. The coefficients in the logarithmic equation of flow resistance were subsequently recalibrated against their experimental data. It was analyzed dimensionally that at high vegetation density, the shear Reynolds number has to be included in the flow resistance law. Jarvela (2005) investigated experimentally the flow resistance above flexible vegetation in an open channel flume using Acoustic Doppler Velocimetry technique and confirmed that the logarithmic velocity profile for smooth open channel flow is altered in vegetated flow and the Darcy-Weisbach's friction factor can be related to the maximum shear stress which occurs approximately at the deflected plant height.

* Corresponding author.
E-mail address: cecwli@polyu.edu.hk (C.W. Li).

http://dx.doi.org/10.1016/j.jher.2014.06.005

Wilson (2007) investigated the variation of hydraulic roughness parameters with flow depth and found that the Manning roughness coefficient increases with decreasing flow depth reaching an asymptotic constant at high submergence depth ratio (water depth to vegetation height). The value of the constant is dependent on the vegetation height and other vegetation properties. Baptist et al. (2007) proposed three equations describing the vegetation induced resistance from different angles. Two equations were based on analytical approach, and one equation was based on analyzing of the synthetic data generated by a 1-D k-ε model using the genetic programming approach.

Nikora et al. (2008) studied the impacts of vegetation on hydraulic resistance and suggested a simple quantitative relation to predict these effects based on flow and vegetation parameters. The analysis showed that the submergence depth ratio is the major parameter to determine hydraulic roughness. Taka-aki and Nezu (2010) examined experimentally the flow structure in an open channel flow with flexible vegetation and confirmed that the zero plane displacement is well correlated with the plant deflected height and that the friction factor increases with the deflected height. Therefore, the mean deflected height was suggested to be a key parameter for hydraulic roughness.

In nature the vegetation parameters have variability which can be described by the mean and covariance. For engineering design and management, it is important to know the variability of the roughness coefficient. There are a lot of methods developed for uncertainty analysis, such as the Monte Carlo method, the Automatic Differentiation technique and the Unscented Transform (UT) method. In the Monte Carlo method a large sample of output data is generated for analysis through the known probability distribution of the input parameters. The computational effort can be substantial. Recently, the UT method has been developed to capture the mean and variance of the output distribution by using the information at multiple points in the input space (e.g., Julier, 2002). The method is derivative-free and requires less function evaluations.

In the present work the numerical modeling approach is used to generate synthetic velocity profile data for hydraulic roughness determination. In the model turbulence is simulated by the Spalart-Allmaras closure with a modified length scale which is dependent on the vegetation density and water depth to vegetation height ratio. Flexibility of vegetation is accounted for by using a large deflection analysis. The model is verified against available experiments. Based on the synthetic data an inducing equation is derived, which relates the Manning roughness coefficient to the vegetation parameters, flow depth and a zero-plane displacement parameter. The derived equation is compared with an existing equation, as well as the data sets of flume experiments conducted by various researchers. The predictive capability of the derived equation is subsequently tested in field conditions. Finally, the uncertainty of the inducing equation is assessed and the UT method is employed to investigate the variability of the Manning roughness due to the propagation of uncertainty from the input parameters. A significant portion of the modeling work has been reported in Busari and Li (2013), the present work provides further verification of the inducing equation and conducts uncertainty analysis of the equation.

2. Numerical model

The numerical model for the determination of hydraulic roughness is based on conservation of mass and momentum of fluid.

Continuity equation:

$$\frac{\partial u_i}{\partial x_i} = 0 \qquad i = 1,2,3 \tag{1}$$

Momentum equation:

$$\frac{\partial u_i}{\partial t} + u_j\frac{\partial u_i}{\partial x_j} = \frac{\partial}{\partial x_j}\left[\nu_m\left(\frac{\partial u_i}{\partial x_j}+\frac{\partial u_j}{\partial x_i}\right)+\frac{\tau_{ij}}{\rho}\right] - \frac{1}{\rho}\frac{\partial p}{\partial x_i} - \frac{1}{\rho}F_i + g_i \qquad i = 1,2,3 \tag{2}$$

where x_i (= x, y, z) are the coordinates in longitudinal, transverse and vertical directions respectively; u_i (= u, v, w) are the time-averaged velocity components in x, y and z directions respectively; t = time; ρ = density of fluid; ν_m = molecular viscosity, $\tau_{ij} = -\rho\overline{u_i'u_j'}$ = Reynolds stresses, F_i(= F_x, F_y, F_z) are the resistance force components per unit volume induced by vegetation in x, y and z directions respectively. $g_i = (0, 0, -9.81\ \mathrm{m/s^2})$ are the components of the gravitational acceleration. The Reynolds stresses are represented by the eddy viscosity model:

$$\frac{\tau_{ij}}{\rho} = -\overline{u_i'u_j'} = \nu_t\left(\frac{\partial u_i}{\partial x_j}+\frac{\partial u_j}{\partial x_i}\right) - \frac{2}{3}\delta_{ij}k \tag{3}$$

where $k = \frac{1}{2}\overline{u_i'u_i'}$ is the turbulent kinetic energy which can be absorbed into the pressure gradient term, ν_t = eddy viscosity. The eddy viscosity ν_t is specified by the Spalart-Allmaras (SA) turbulence model which involves the solution of a new eddy viscosity variable ν. The version of the model used is for near-wall region and finite Reynolds number, which is most relevant to the present problem (Spalart and Allmaras, 1994).

$$\frac{\partial \nu}{\partial t} + u_j\frac{\partial \nu}{\partial x_j} = c_{b1}\tilde{S}_\nu\nu + \frac{1}{\sigma}\left\{\frac{\partial}{\partial x_j}\left[(\nu+\nu_m)\left(\frac{\partial \nu}{\partial x_j}\right)\right] + c_{b2}\left(\frac{\partial \nu}{\partial x_j}\frac{\partial \nu}{\partial x_j}\right)\right\} - c_{w1}f_w\left(\frac{\nu}{d}\right)^2 \tag{4}$$

where

$$\nu_t = \nu f_{\nu 1}, \quad \tilde{S}_\nu = S_\nu + \frac{\nu}{\kappa^2 d^2}f_{\nu 2}, \quad S_\nu = \sqrt{\omega_j\omega_j}, \quad \chi = \frac{\nu}{\nu_m}$$

$$f_{\nu 1} = \frac{\chi^3}{\chi^3 + c_{\nu 1}^3}, \quad f_{\nu 2} = 1 - \frac{\chi}{1+\chi f_{\nu 1}}, \quad f_w = g\left[\frac{1+c_{w3}^6}{g^6+c_{w3}^6}\right]^{1/6}$$

$$g = r + c_{w2}\left(r^6 - r\right), \quad r = \frac{\nu}{\tilde{S}_\nu\kappa^2 d^2}$$

where, c_{w2} and c_{w3} are constants (see nomenclature).

$S_v = \sqrt{\omega_j \omega_j}$ = magnitude of the vorticity, κ = von Karman constant and d = length scale.

$c_{w1} = \frac{c_{b1}}{\kappa^2} + \frac{1+c_{b2}}{\sigma}$. This turbulence model is a one-equation model which is simpler than the commonly used k-ε or k-ω model and it has been successfully applied in the modeling of certain free-shear flow, wall-bound flow and separated flow problems. The resistance force due to vegetation is determined by the quadratic friction law. The average force per unit volume within the vegetation domain is obtained by.

$$F_i = \frac{1}{2}\rho C_D b_v N u_i \sqrt{u_j u_j} \quad i = 1,2 \tag{5}$$

where C_D = drag coefficient of stem.

For wall bounded shear flow, the turbulence length scale d is proportional to the distance from the point of interest to the channel bed. In the presence of vegetation, the turbulence eddies above the vegetation canopy may not reach the channel bed and thus the turbulence length scale will be reduced. One approach to model the reduction in the turbulence length scale is to set a zero plane displacement parameter z_0. The proposed turbulence length scale of a point at level z is given by.

$$\begin{array}{ll} L = Z - Z_0 & Z > k_d > Z_0 \\ L = Z(k_d - Z_0)/k_d & Z < k_d \end{array} \tag{6}$$

where k_d = deflection vegetation height.

Natural vegetation bends in high flow and the horizontal deflection at the top of a vegetation stem can be of the same order as the deflected stem height. Hence, the classical small deflection theory of a beam may not be adequate for a vegetation stem with high flexibility. In this study, a large deflection analysis based on the Euler-Bernoulli law for bending of a slender beam has been used to describe the deflection of a vegetation stem (Li and Xie, 2011). In the analysis each vegetation stem is modeled as a vertical in-extensible non-prismatic slender beam of length l. The water flow produces variable distributed loads $q_x(s)$ on the beam along the x-direction as shown in Fig. 1. Combining the Euler-Bernoulli law for the local bending moment and the equations of the equilibrium of forces and moments, the following fourth order nonlinear equation in the deflection δ is obtained.

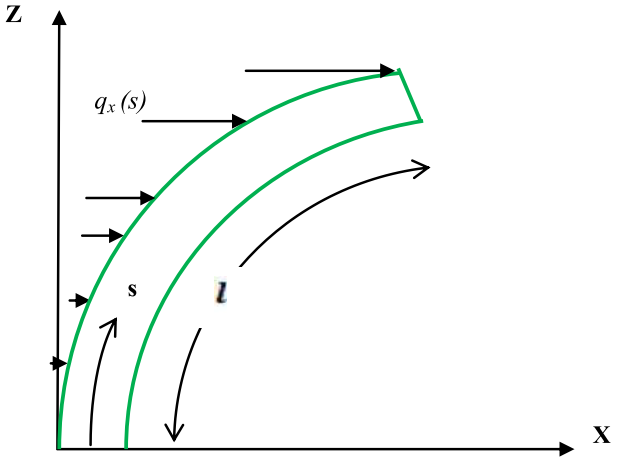

Fig. 1. Schematic diagram of large deflection of a beam carrying distributed load.

$$\frac{d^2}{ds^2}\left[EI(s)\frac{\frac{d^2\delta}{ds^2}}{1-\left(\frac{d\delta}{ds}\right)^2}\right] + \frac{d}{ds}\left[EI(s)\frac{\frac{d^2\delta}{ds^2}}{1-\left(\frac{d\delta}{ds}\right)^2}\right]\frac{\frac{d\delta}{ds}\frac{d^2\delta}{ds^2}}{1-\left(\frac{d\delta}{ds}\right)^2} = -q_x(s)\sqrt{1-\left(\frac{d\delta}{ds}\right)^2} \tag{7}$$

where s = local ordinate along the beam, E = flexural stiffness, I = second moment of area and δ = deflection in x-direction. The vegetation stem is taken as inextensible as the total length remains constant. By dividing the stem into n equal part of constant length Δs, the z-ordinate of the i th node is obtained by

$$z_i = \sum_{j=1}^{i} \sqrt{\Delta s^2 - (\delta_i - \delta_{i-1})^2} \tag{8}$$

The deflected height of the stem is then equal to z_n. Equation (7) is solved by using a quasi-linearized central finite difference scheme. To save computational effort, the solution is expressed in non-dimensional form relating the deflected height to the applied force, and is approximated by a polynomial. Details can be found in Li and Xie (2011).

Under uniform flow condition, the problem becomes one-dimensional and the 1D version of the numerical model by Li and Zeng (2009) can be used. The flow variables are the longitudinal velocity component u_1 and the eddy viscosity, varying along the vertical direction. The boundary conditions are as follows. At the free water surface the normal gradients of the variables are zero. At the bottom the velocity is determined by the wall function and the eddy viscosity is determined by the mixing length hypothesis.

3. Model verification

Four cases have been chosen for the verification of the numerical model. The flow and vegetation parameters for the experiments are shown in Table 1. The number of grids used is 61 and the time step size is in the order of 0.0005s to ensure computational stability. Grid convergence study shows that further reduction of grid size does not affect the results apparently.

Fig. (2) shows the comparison between the numerical results and the experimental data of rigid vegetation of Lopez and Garcia (2001). The computed velocity profile above the vegetation layer agreed well with that reported in the experiment. The difference between the presently computed velocity above vegetation and the corresponding measured value is less than 7%. Similar accuracies are obtained for the simulation of the experimental cases of both rigid and flexible vegetation due to Dunn et al. (1996), as shown in Fig. (3).

Table 1
Flow and vegetation parameters of cases for numerical model verification.

Investigator	Run	N(m^{-2})	h(m)	k_v(m)	b_v(mm)	Type	u_m(m/s)	S (%)
Lopez and Garcia (2001)	Exp. 1	142	0.335	0.12	6.35	Rigid	0.876	0.36
Jarvela (2005)	R4-8	12,000	0.707	0.26	2.80	Flexible	0.129	0.02
	R4-9	12,000	0.704	0.22	2.80	Flexible	0.185	0.03
Wilson (2007)	A-2	833,333	0.04–0.17	0.016		Flexible	0.13–0.35	0.10
Dunn et al. (1996)	2	172	0.229	0.118	6.35	Flexible	0.422	0.36
	6	43	0.267	0.118	6.35	Flexible	0.733	0.36
	13	172	0.368	0.152	6.35	Rigid	0.536	0.36
	15	43	0.257	0.132	6.35	Rigid	0.398	0.36

h = water depth, u_m = mean velocity, S = channel bottom slope.

The computed and measured velocity profiles for the cases of Wilson (2007) are shown in Fig. (4). The flexibility of the grass was not determined in the experiments. In the numerical simulation the flexural rigidity of grass was calibrated to reproduce the observed deflected height. The profile is in non-dimensional form and is obtained by combining the results of several experiments with different h/k_v ratios. The computed results and measured data are almost overlapping. The results show a good correlation of the trend of variation of the velocity with h/k_v ratio within the range of selected water depth.

Fig. (5) displays the computed and measured velocity profiles for the case of Jarvela (2005). The shear velocity is defined using the clear water depth (equal to total water depth minus the vegetation height), which is the same as that adopted by Jarvela (2005). The computed results are in good agreement with the measured data in the clear water zone and exhibit a low velocity region in the vegetation layer. There was no data recorded within the vegetation region, primarily due to the high vegetation density.

The vegetation induced roughness can be expressed in terms of the Manning coefficient through the Manning equation for uniform flow. The capacity of the numerical model in predicting the vegetation induced roughness effect is examined in 117 cases with available experimental data. The data were measured in laboratory flumes, covering a wide range of vegetation parameters and flow depths, and were reported in six independent literature (Ikeda, 1996; Poggi et al., 2004; Jarvela, 2005; Carollo et al., 2005; Velasco et al., 2008; Zeng, 2011). In the computations, for cases in which the drag coefficient is not specified, the value of 1.2 is adopted. If the deflected height of vegetation is not specified, it will be computed using the large deflection analysis described above. The zero-plane displacement has been fine tuned to give the best fit result. The values of the Manning coefficient derived from the experimental data are compared with the calculated values using the model. Fig. (6) shows the well agreement between the computed values and the measured data, with the difference generally within 10%.

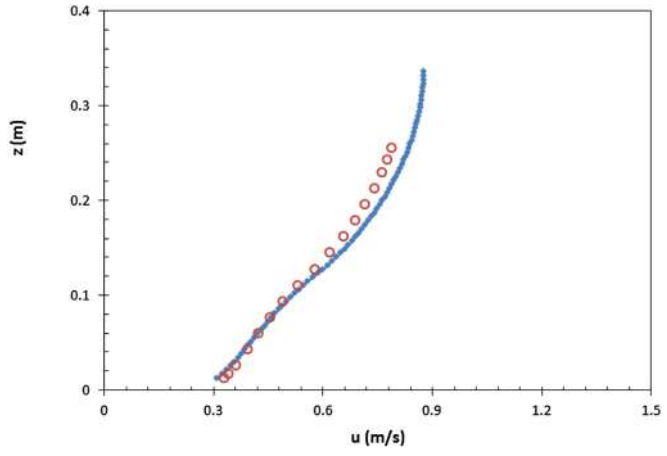

Fig. 2. Velocity profile comparison for Lopez and Garcia, (2001). Solid line – computed; circle – measured.

4. Inducing equations

4.1. Fitting equations

Numerical experiments have been carried out against available experimental data to obtain an empirical equation of z_o which is given by.

$$\frac{z_0}{k} = \frac{f_v^{\beta}}{f_v^{\beta} + \alpha^{\beta}} \tag{9}$$

where f_v is the vegetative resistance parameter ($= C_D N b_v k_v$), α and β are constants. The equation is in reasonable agreement with the equation proposed by Raupach (1994).

Several empirical equations for vegetation induced roughness have been proposed previously, including Kouwen and Unny (1973) for flexible vegetation, Baptist et al. (2007) and Gu (2007) for rigid vegetation. The equations are of the following general form.

$$n = \frac{h^{1/6}}{\sqrt{g}[a + b\log(h/k_s)]} \tag{10}$$

where a, b are parameters dependent on the flow and vegetation parameters; k_s is a roughness parameter. In this study a refined empirical equation for vegetal roughness is derived from the numerical model generated synthetic data and will be compared with the other available equations. After extensive tests the following equation is proposed.

$$n = \frac{h^{1/6}}{\sqrt{\frac{2g}{f_v}} + A'\frac{\sqrt{g}}{\kappa}\ln\left(\frac{h - z_0'}{k_v - z_0'}\right)} \tag{11}$$

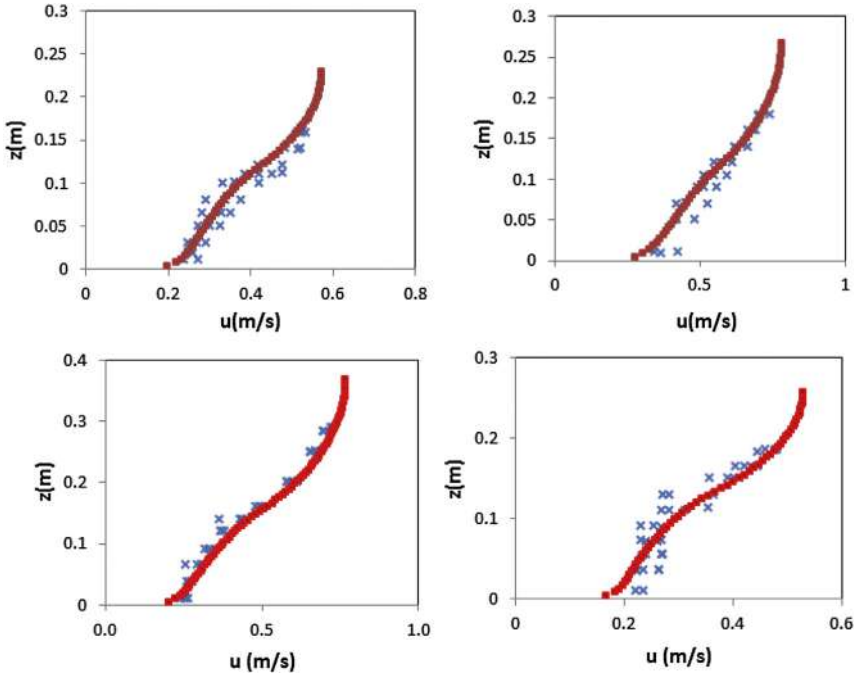

Fig. 3. Velocity profile comparison for Dunn et al. (1996). Run 2 and 6 (top row) for rigid vegetation; Run 13 and 15 (bottom row) for flexible vegetation. (Cross – measured; solid line – computed).

where A' is an empirical parameter and $\kappa = 0.41$. The parameter, Z_o' represents a modified zero plane displacement parameter and is given by

$$z_0' = z_0 \exp\left(\frac{-\eta}{f_v^{3/4}}\right) \tag{12}$$

where $\eta = 3.7$. Numerical simulations show that the parameter 'A' is a nonlinear function of h/k_v. The fitting of eq. (12) to the synthetic data from numerical simulations leads to the following quartic polynomial equation.

$$A'\left(\frac{h}{k_v}\right) = a_1\left(\frac{h}{k_v}\right)^4 + a_2\left(\frac{h}{k_v}\right)^3 + a_3\left(\frac{h}{k_v}\right)^2 + a_4\left(\frac{h}{k_v}\right) + 0.6026 \tag{13}$$

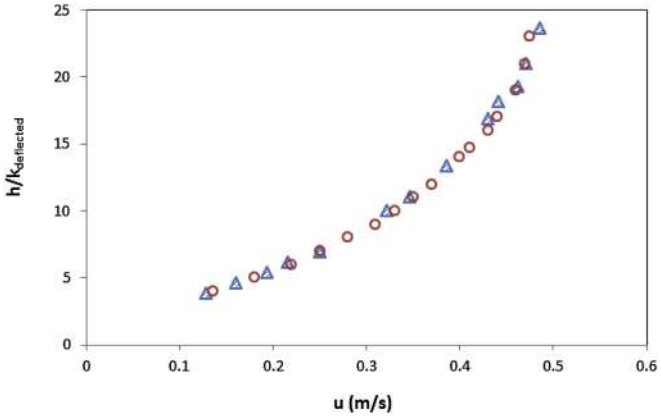

Fig. 4. Velocity profile comparison for Wilson, (2007). Circle – computed; Triangle – measured.

where a_1, a_2, a_3 and a_4 are constants equal to *0.0043*, *−0.0608*, *0.2550* and *−0.1604* respectively. The correlation coefficient of the fitting is high and is equal to 0.991. Fig. (7) shows that the fitting is the best at lower values of h/k_v, and has larger discrepancy when f_v is low and h/k_v is high (i.e. in the low hydraulic resistance range).

A simplified form of equation (11) can be obtained by noting that the exponential function in equation (12) approaches 1 at very high vegetation density ($f_v \to \infty$). In that case $z_o' \to z_0$, and equation (11) takes the following form:

$$n = \frac{h^{1/6}}{\sqrt{\frac{2g}{f_v}} + A\frac{\sqrt{g}}{\kappa}\ln\left(\frac{h-z_0}{k_v-z_0}\right)} \tag{14}$$

The fitting of equation (14) to the synthetic data yields a quadratic polynomial equation of A and h/k with correlation coefficient approximately equal to 1. The equation is given by:

$$A\left(\frac{h}{k_v}\right) = b_1\left(\frac{h}{k_v}\right)^2 + b_2\left(\frac{h}{k_v}\right) + 0.3951 \tag{15}$$

where b_1 and b_2 equal to 0.0165 and 0.0379 respectively.

4.2. Verification of equations

Equations (11) and (14) are then verified by the experimental data and compared with the equation proposed by Baptist et al. (2007). The available experiments are subdivided into three categories with different vegetation densities and submergence. A brief description of the parameters of the data sets is shown in Table 2. In parallel the inducing equation by Baptist et al. (2007) is also employed for comparison. The

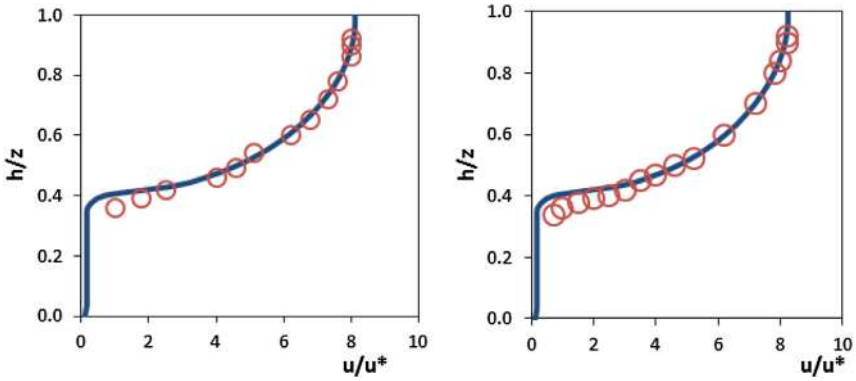

Fig. 5. Velocity profile comparison for Jarvela, (2005). Run R4-8 (left), Run R4-9 (right). Solid line – computed; circle – measured.

equation is as follows and is simpler than equations (11) and (14), but the zero plane displacement parameter is not included.

$$n = \frac{h^{1/6}}{\sqrt{\frac{2g}{f_v}} + \frac{\sqrt{g}}{\kappa}\ln\left(\frac{h}{k_v}\right)} \tag{16}$$

For *category I* in which the vegetation density is low, the vegetation is artificial and is either rigid or flexible. The comparison results are presented in Fig. (8), showing good agreement between the empirical equations and the experimental data. equation (11) gives the best fit results.

Category II consists of data corresponding to natural or artificial vegetation with medium density and wider range of degree of submergence. The results in Fig. (9) show that the equations generally yield good results comparing with the experimental data. equation (16) overestimates the Manning roughness at higher vegetation density whereas equation (14) produces wider scattering of the results around the line of perfect agreement.

In *category III*, the vegetation is natural and of very high density, ranging from 28,000 to 44,000 stems/m^2. In the simulation it was found that the drag coefficient needed to be adjusted to 0.1 due to the large deflection of the plants and the significant sheltering effect induced. Fig. (10) shows that the results computed by equation (11) and equation (16) bias on the high side and overestimates the Manning's roughness coefficient. The degree of scatter increases with decreasing Manning roughness coefficient. equation (14), however, gives good prediction results. This is mainly because the zero plane displacement z_o is important for these cases with high vegetation density. Water flow is significantly retarded by the vegetation and the turbulence eddies cannot penetrate into the lower vegetation region. equation (14) is most sensitive to the change in z_o.

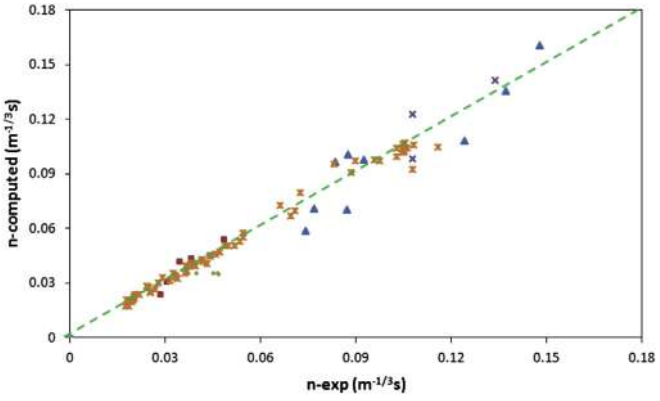

Fig. 6. Comparison between the measured values and computed values of Manning coefficient +; Ikeda and Kanazawa (1996); □ Poggi et al. (2004); △; Jarvela (2005); *; Carollo et al. (2005); –;Velasco et al. (2008); × Zeng (2011)

4.3. Further verification of equations

Recently, two new hydraulic roughness models for vegetated flows were proposed by Yang and Choi (2010) and Cheng (2011). They were both developed using the concept of two-layer approach to the velocity profile of vegetation flow. The equation due to Yang and Choi (2010) is:

$$n = \frac{h^{1/6}}{\sqrt{\frac{2g}{f_v}} + \frac{1}{\kappa}\sqrt{\frac{g(h-k_v)}{h}}\left[C_u \ln\left(\frac{h}{k_v}\right) - \left(\frac{h}{k_v} - 1\right)\right]} \tag{17}$$

where $C_u = 1$ for $Nb_v \leq 5\ \mathrm{m}^{-1}$ and $C_u = 2$ for $Nb_v > 5\ \mathrm{m}^{-1}$. The simplified form of the equation due to Cheng (2011) is:

$$n = \frac{h^{1/6}}{\sqrt{\frac{g(4-\varsigma)^3}{32 f_v}\left(\frac{k_v}{h}\right)^{1.5} + \frac{C\sqrt{g}}{\kappa}\left[\left(\frac{h-k_v}{b_v}\right)\left(\frac{4}{\varsigma} - 1\right)\right]^{0.0625}\left(1 - \frac{k_v}{h}\right)^{1.5}}} \tag{18}$$

where C = 1.8614 and $\varsigma = N\pi b_v^2$

The proposed empirical equation (equation (14)) is further compared with the equations above using a large set of experimental data from nine investigators (Cheng, 2011). The results are shown in the Fig. (11) and Fig. (12) for rigid vegetation and flexible vegetation, respectively. For flexible vegetation in Fig. (12), the value of C_D is computed by using the empirical equation due to Cheng (2011). The figures depict that the three equations are of similar accuracies in predicting

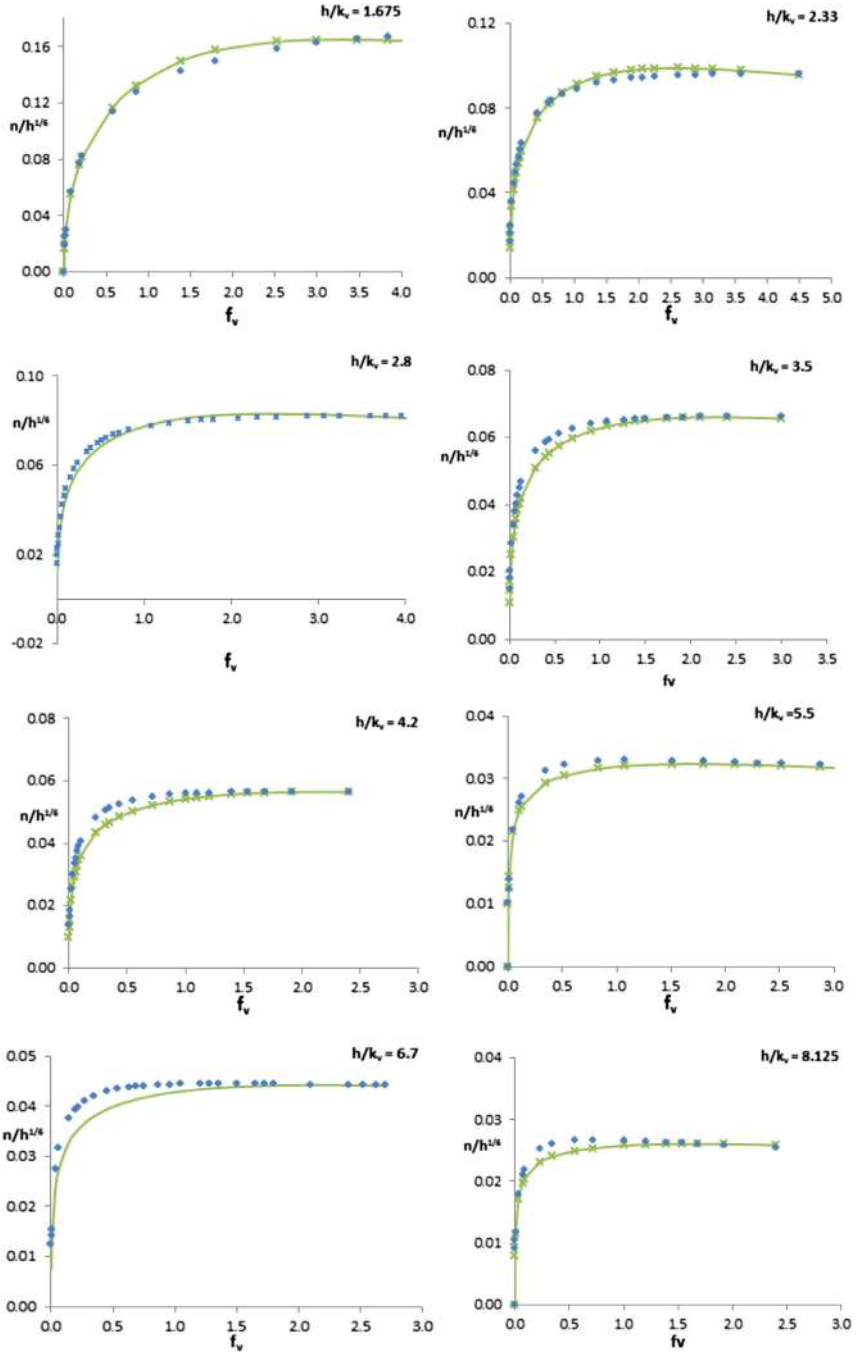

Fig. 7. Fitting equation (11) and synthetic data for different submergence ratio (Blue dots denote synthetic data; green line – fitting equation). (For interpretation of the references to color in this figure legend, the reader is referred to the web version of this article.)

the Manning roughness for rigid vegetation, while the proposed equation yields better results for cases with highly flexible vegetation.

4.4. Field application

While most empirical equations were validated against laboratory measurement data only (e.g. Klopstra et al., 1997; Stephan and Gutknecht, 2002; Brian and Shen, 2002; Gu, 2007 and Baptist et al., 2007), the present study extends the validation study against field data. Nikora et al. (2008) studied the impacts of aquatic vegetation on hydraulic resistance in five small streams and suggested empirical equations to predict these effects. The reach length of stream considered varied from 12 to 30 m. The dominant vegetation types of varying flexibility and variable morphology under consideration were Charophytic alga (Nitella hookeri), Myriophyllum sp., Riccia sp., Filamentous algae and Elodea canadensis.

Table 2
A list of the datasets used in the verification of inducing equation.

Investigator(s)	Category	N(m^{-2})	h/k_v	Vegetation characteristics
Lopez and Garcia (2001)	I	≤500	$1.2 \le h/k \le 3.5$	Artificial, rigid wooden dowels.
Huai et al. (2009)				Artificial, rigid metal rods.
Velasco et al. (2008)				Artificial, flexible plastic strips.
Zeng (2011)				Artificial, flexible plastic strips.
Ikeda and Kanazawa (1996)	II	≤15,000	$1.4 \le h/k \le 5.0$	Artificial, flexible Nylon filaments.
Poggi et al. (2004)				Artificial, rigid stainless steel.
Jarvela (2005)				Natural, flexible wheat.
Velasco et al. (2008)	III	≥2,0000	$1.6 \le h/k \le 9.0$	Natural, flexible Barley grass.
Carollo et al. (2002)				Grass mixture.
Carollo et al. (2005)				Grass mixture.

In the simulation the parameter f_{rk} $(= C_D b_v N)$ is not available and needs to be estimated. The drag coefficient C_D is in the order of 1, the exact value depends on the streamlined flow effect due to vegetation deflection. The stem width b_v lies between 4 and 6 mm and the density N depends on the plant characteristics (Bowmer et al., 1995; Hofstra et al., 2006; Kevin et al., 2007). In the simulation, the average stem width is taken to be 5 mm for all vegetation types, the vegetation density is assumed to be 12,000/m^2. Figure (13) showed that the computed Manning's coefficients are in good agreement with the measured datasets reported by Nikora et al. (2008). The predicted value of the Manning's coefficient is found not quite sensitive to the value of f_{rk} within the practical range.

5. Uncertainty analysis of vegetated flow modeling

5.1. Uncertainties of input parameters and fitting equations

For engineering design and management of vegetated channels, it is important to estimate the uncertainty of the hydraulic conditions of the channels. The Manning roughness coefficient is one of the key parameters needed to be investigated. It is affected by the vegetation parameter as well as the flow conditions. In the field, the uncertainty in the vegetative parameters is largely due to the natural variability of the vegetation characteristics. For example, the seasonal/time variation in the growth of plant can affect the flexural rigidity and plant height; the spatial variation of plants may affect the density and stem diameter. This type of (aleatory) uncertainty cannot be eliminated. In laboratory experiments, this source of uncertainty is not significant as identical simulated vegetation elements are generally used. In addition, the formulation of the induced equations relating the input vegetation and flow parameters to the hydraulic roughness coefficient will have uncertainty. In the present study the two sources of uncertainty are considered as a whole. The computed values of the Manning roughness coefficient are compared with the corresponding measured data. Table (3) summarizes the estimated errors induced by equations (11), (14) and (16)–(18). The errors are computed by using the Normalized Root Mean Square Deviation (NRMSD) method which is defined as.

$$NRMSD = RMSD/(n_{measured,max} - n_{measured,min})$$
$$RMSD = \sqrt{\frac{1}{m}\sum_{j=1}^{m}\left(n_{measured,j} - n_{computed,j}\right)^2} \quad (19)$$

The normalization using the range of measured Manning's roughness is considered more reasonable than that using the mean value due to the high degree of variability in the data, especially for the field data. On average, the equations proposed by Baptist et al. (2007), Cheng (2011) and Yang and Choi (2010) and the present study appear to be more accurate for rigid vegetation. equations (16) and (18) appear to be less accurate for flexible vegetation. The proposed equations (11) and (14) in the present study perform almost the best. Generally, the equations perform worse for cases requiring

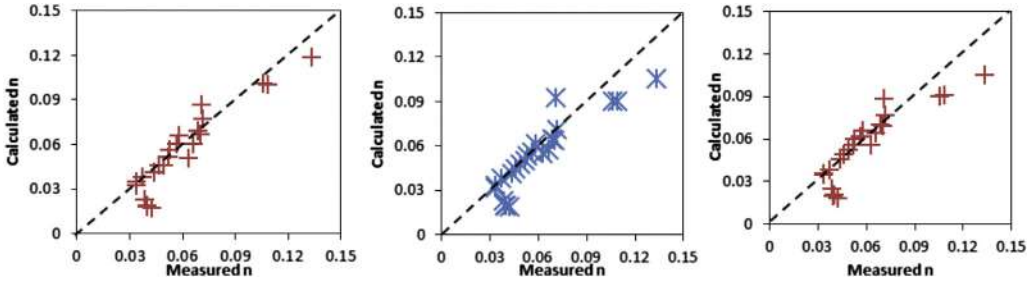

Fig. 8. Comparison between the measured values of n ($m^{-1/3}$s) and those calculated using equation (11) (Left), equation (14) (Right) and equation (16) (Middle) for Category I cases.

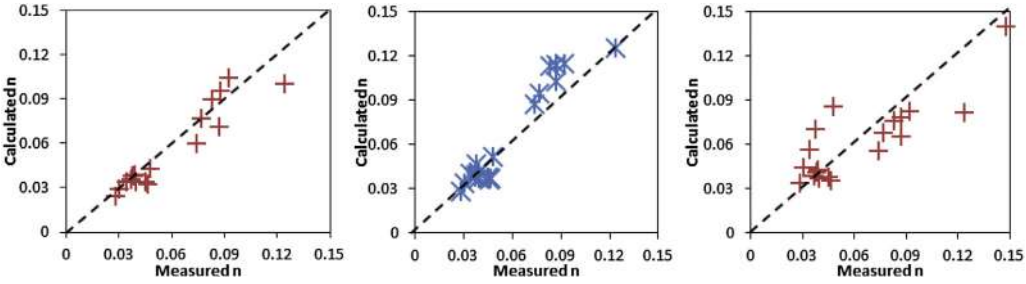

Fig. 9. Comparison between the measured values of n ($m^{-1/3}s$) and those calculated using equation (11) (Left), equation (14) (Right) and equation (16) (Middle) for Category II cases.

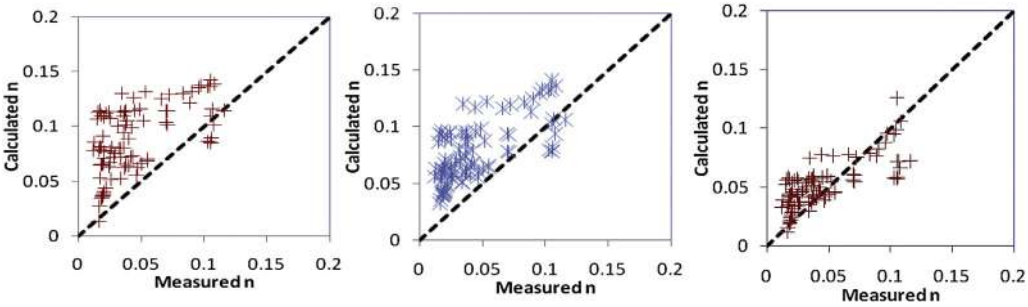

Fig. 10. Comparison between the measured values of n ($m^{-1/3}s$) and those calculated using equation (11) (Left), equation (14) (Right) and equation (16) (Middle) for Category III cases.

estimation of the drag coefficient. The estimated NRMSD uncertainty using the present fitting equations are less than 18% for the entire verification stage.

5.2. Propagation of uncertainty – unscented transformation (UT)

UT is a deterministic method to obtain the statistical properties (mean and covariance) of an output variable (Manning roughness) subjected to a nonlinear transformation through the numerical model or the inducing empirical equation. The statistical properties (mean and covariance) of the input parameters are specified, either obtained from measurements or from design requirements. A set of sigma points for the input parameters are then chosen and the corresponding output points are computed. The statistical properties of the output parameter are obtained through a linear combination of the output points with appropriate weightings. The basic idea

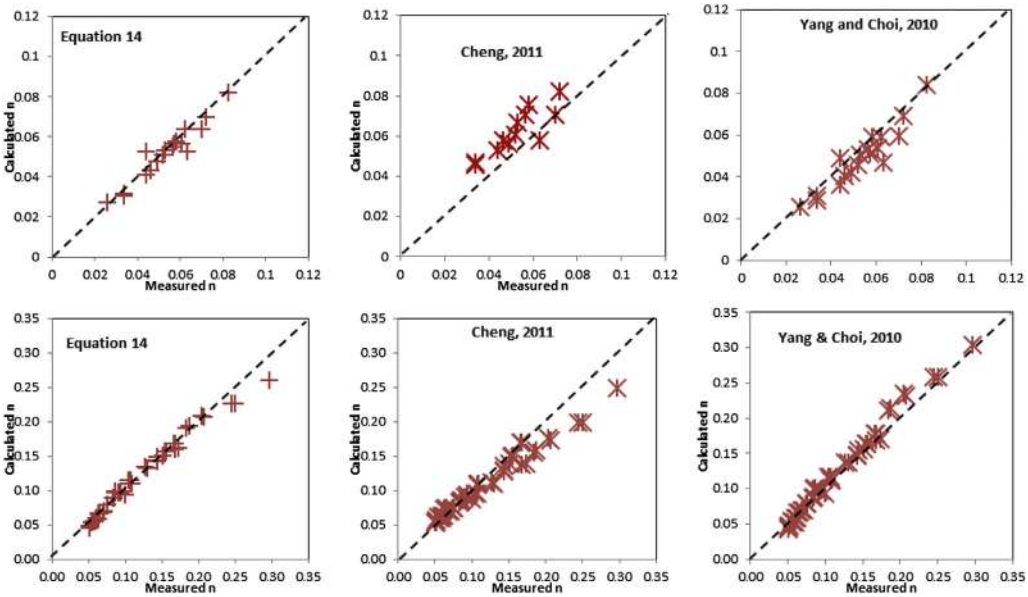

Fig. 11. Vegetative Manning's roughness, n ($m^{-1/3}s$) comparison, (top row) for Dunn et al. (1996) and (bottom row) for Meijer (1998).

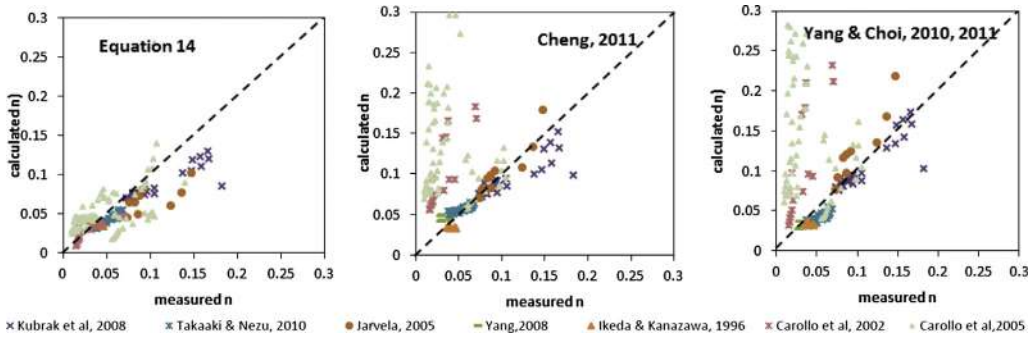

Fig. 12. Vegetative Manning's roughness, n ($m^{-1/3}s$) comparison for highly flexible vegetation.

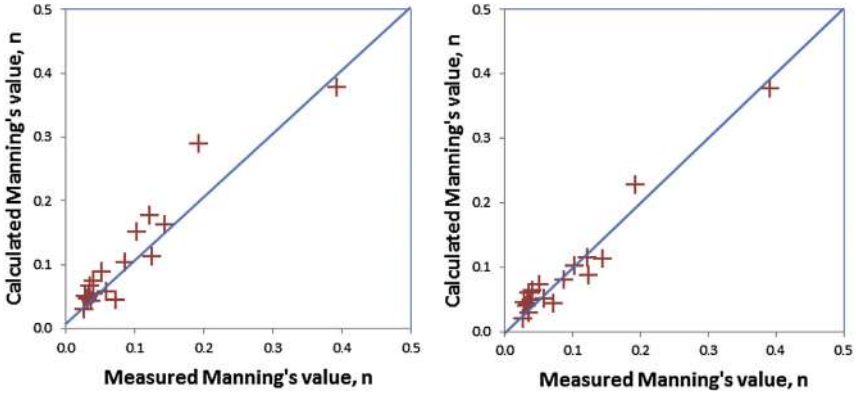

Fig. 13. Field verification of equation (11) (left) and equation (14) (right).

Table 3
NRMSD (%) generated by different empirical equations (nc = number of cases).

Verification stage	Investigators	Equation	Manning coefficient (%)	Reference
1.	Baptist et al. (2007)	16	13.2	Fig. 8 ($nc = 23$)
		14	12.6	
	Present study	11	11.1	
	Present study			
	Baptist et al. (2007)	16	16.9	Fig. 9 ($nc = 21$)
		14	18.8	
	Present study	11	15.9	
	Present study			
	Baptist et al. (2007)	16	56.2	Fig. 10 ($nc = 105$)
		14	25.5	
	Present study	11	49.8	
	Present study			
2.	Baptist et al. (2007)	16	8.8	Fig. 11 ($nc = 60$)
		17	7.2	
	Yang and	18	8.7	
	Choi, (2010)	14	8.0	
	Cheng, 2011	11	8.1	
	Present study			
	Present study			
	Baptist et al. (2007)	16	94.5	Fig. 12 ($nc = 172$)
		17	26.7	
	Yang and	18	136	
	Choi, (2010)	14	14.8	
	Cheng, 2011	11	16.1	
	Present study			
	Present study			
3	Present study	14	7.4	Fig. 13 ($nc = 18$)
	Present study	11	9.6	

of the method is that the statistical parameters of an output variable can be more conveniently obtained from the nonlinear transformation of the statistical parameters of the input variables. The method requires less function evaluations and is considered better than the Monte Carlo simulation method in terms of flexibility, ease of implementation and practicability (Padulo et al., 2007; Menezes et al., 2013; Stéphanie et al., 2013).

In UT the m-dimensional random variable $\boldsymbol{x}$ with mean $\bar{x}$ and covariance Σ is approximated by $2m + 1$ weighted samples or sigma points of locations x_i and weights W_i based on the following constraints.

$$\begin{aligned}
&\sum_{i=0}^{2m} W_i = 1\\
&\sum_{i=0}^{2m} W_i x_i = \bar{\boldsymbol{x}}\\
&\sum_{i=0}^{2m} W_i (x_i - \bar{\boldsymbol{x}})(x_i - \bar{\boldsymbol{x}})^T = \sum_x
\end{aligned} \tag{20}$$

The sigma points thus are not unique and one commonly used set is as follows.

$$\begin{aligned}
&x_o = \hat{\boldsymbol{x}} = \mu\\
&x_i = \mu + \left(\sqrt{(m+\lambda)\,\Sigma}\right)_i = \mu + \alpha_o\sqrt{(m+\varpi)}\sigma_i \quad i = 1, \ldots, m\\
&x_i = \mu - \left(\sqrt{(m+\lambda)\,\Sigma}\right)_i = \mu - \alpha_o\sqrt{(m+\varpi)}\sigma_i \quad i = m+1, \ldots, 2m
\end{aligned} \tag{21}$$

Table 4
Uncertainty propagation analysis: mean.

Test case	σ	Exact solution	UT method	Relative uncertainty (%)	Mean $E(\boldsymbol{n})$
		Mean ($\overline{n}$)	Mean ($\boldsymbol{n}_{UT}$)		
Equation 11	0.20	0.1219	0.1219	0.00	0.122
	0.15	0.1208	0.1221	1.07	
	0.10	0.1221	0.1223	0.16	
	0.05	0.1224	0.1224	0.00	
Equation 14	0.20	0.1149	0.1149	0.00	0.115
	0.15	0.1141	0.1152	0.96	
	0.10	0.1152	0.1154	0.17	
	0.05	0.1155	0.1155	0.00	

The weights for computing the mean, $W_i^{[\mu]}$ and covariance, $W_i^{[c]}$ are

$$W_0^{[\mu]} = \frac{\lambda}{m+\lambda}$$
$$W_i^{[\mu]} = W_i^{[c]} = \frac{1}{2(m+\lambda)} \text{ for } i = 1, \ldots, 2m \quad (22)$$
$$W_i^{[c]} = W_0^{[\mu]} + \left(1 - \alpha_o^2 + \beta_o\right)$$

where λ, ϖ, α_o, β_o are scaling parameters (Van der Merwe, 2004; Kim and Park, 2010), m is the dimensionality and $\left(\sqrt{(m+\lambda)\,\Sigma}\right)_i$ is the ith column of the matrix square root of $(m+\lambda)\ \Sigma$. The optimum choice of scaling parameters is: $0 < \alpha_o < 1$; $\beta_o = 2$; $\varpi > 0$, and $\lambda = \alpha_o^2(m+\varpi) - m$.

After transformation mapping f, the estimated mean and covariance of the output variable are obtained by:

$$\mu' = \sum_{i=0}^{2m} W_i^{\mu} f\left(x^{[i]}\right)$$
$$\Sigma' = \sum_{i=0}^{2m} W_i^{c} \left(f\left(x^{[i]}\right) - \mu'\right)\left(f\left(x^{[i]}\right) - \mu'\right)^T \quad (23)$$

In case the number of input parameters is small (say 2) the analytical solution of the mean and covariance of the output variable can be computed easily, knowing that the probability distribution is a normal distribution. Following Padula et al. (2007), the fitting equations (11) and (14) are used to illustrate the accuracy of the UT method. The input variables chosen are f_v ($= C_D N b_v k_v$) and plant height k_v. They are both assigned the same mean value of 1, same standard deviation σ ($= 0.05, 0.1, 0.15, 0.2$) and zero cross covariance for simplicity. The water depth was assumed uniform. The average stem width of 4 mm was selected, assuming a very flexible vegetation with $C_D = 0.5$. The vegetation is totally submerged.

Table 5
Uncertainty propagation analysis: covariance.

Test case	σ	Exact solution	UT method	Relative uncertainty (%)
		Covariance	Covariance	
Equation 11	0.2	6.777e-4	6.799e-4	0.3246
	0.15	3.763e-4	3.876e-4	3.0029
	0.1	1.721e-4	1.737e-4	0.9297
	0.05	4.359e-5	4.361e-5	0.0459
Equation 14	0.2	3.997e-4	4.029e-4	0.8006
	0.15	2.112e-4	2.172e-4	2.8409
	0.1	9.281e-5	9.371e-5	0.9697
	0.05	2.299e-5	2.302e-5	0.1305

Table 6
Measured parameters (Boller and Carrington, 2006).

	k_v	b_v	$C_{D(hv)}$	$C_{D(lv)}$
Mean	0.0735	0.0424	0.265	0.594
Covariance	0.0003	0.0001	0.0071	0.0359
CoV	0.222	0.225	0.318	0.319

The computed results are shown in Table 4 and Table 5. The difference between the computed and exact mean and covariance values is around 1% and 3% respectively. The estimated mean values of the output variable (Manning roughness coefficient) for the two equations using the mean values ($\boldsymbol{x}_o$) of the input parameters are also included in Table 4 and denoted by $E(n)$. These mean values are commonly taken as the expected value of the output parameter if no information about the covariance is given. It can be seen that this method is slightly less accurate than the UT method as the information of covariance is not used.

The UT method is then used to study the uncertainty of the Manning roughness coefficient induced by the propagation of the variability of shape and flexibility of vegetation during reconfiguration. Boller and Carrington (2006) conducted hydrodynamic experiments of 19 samples of macro-alga to determine their drag characteristics. The measured parameters are shown in Table 6, where $C_{D(hv)}$ = drag coefficient in high velocity condition ($u = 1.9$ m/s); $C_{D(lv)}$ = drag coefficient in low velocity condition ($u = 0.5$ m/s). The data are sparse and the distribution does not strictly follow the normal distribution. In the test case, the water depth is assumed to be approximately uniform ($h = 0.15$ m), the vegetation density is set to 1000. The dimensionality of the problem is $m = 3$ and 7 sigma points are required. The sigma points are computed using equations (20)–(22).

The analysis is carried out for the two flow regimes. The computed results by UT using equation (14) and the 7 sigma points are shown in Table 7. The computed coefficient of variation (CoV) for both cases is around 0.2, showing that the Manning roughness can have a significant variation arising from the variability in the vegetation parameters. The computed Manning roughness coefficient for the case using the mean values ($\boldsymbol{x}_o$) of the input parameters is 2–5% lower

Table 7
Computed Manning's roughness coefficient by Eq. (14) based on UT.

	Mean	Variance	CoV	x_o
Low velocity (0.5 m/s)	0.0721	0.00025	0.219	0.0760
High velocity (1.9 m/s)	0.0710	0.00022	0.209	0.0721

than that computed by UT. This indicates that the dispersion of the input parameters exerts an effect on the mean output values. The commonly used method of estimating the mean Manning roughness coefficient using the mean vegetation and flow parameters will have errors.

6. Discussion and conclusion

For submerged vegetated flows, the characteristics of flows within the vegetation layer and the clear water layer can be distinctively different. Part of the flow in the clear water layer will penetrate into the vegetation layer. The depth of penetration will depend on the vegetation characteristics and flow conditions. The turbulence length scale within the vegetation layer and that within the clear water layer are also different. To differentiate this difference in turbulence characteristics and to account for the resulting hydraulic resistance effect, a zero-plane displacement parameter (z_o) is introduced into an inducing equation and its simplified form for submerged vegetated flows. The new inducing equations are calibrated from the synthetic velocity profile data generated by a numerical model which has been extensively verified. The zero-plane displacement parameter is shown to relate empirically with the vegetation parameters through equations (9) and (12). A large number of experimental data sets by various investigators are then used to verify the equation and its simplified version. The vegetation tested ranges from natural to artificial type, with low to high density, and with rigid to highly flexibility. The performance of the equations is generally better than previous equations without the zero plane displacement parameter. The equations have been subsequently applied to the field successfully.

For practical applications, the accuracy of the prediction by the equations is further assessed. The sources of uncertainty are due to the limitations of the equations and the variability of the input vegetation and flow parameters. The uncertainty of the inducing equations in the estimation of the Manning roughness coefficient is expressed by the NRMSD and is found to be less than 18% for the entire data set. The prediction accuracy is higher if the drag coefficient is measured and specified. The propagation of the uncertainty due to the variability of the vegetation and flow parameters existed in nature is investigated by using the method of UT. The method is found efficient and gives a more accurate estimation of the mean Manning roughness coefficient. By measuring the vegetation and flow parameters with uncertainty ranges, the inducing equations together with the UT method can be used to compute the mean and covariance of the Manning roughness coefficient.

Acknowledgment

This work is supported by the Research Grant Council of the Hong Kong Special Administrative Region under Grant No. 5200/12E and a grant from the Hong Kong Polytechnic University.

Nomenclature

c_{b1}	constant (= 0.1355)
c_{b2}	constant (= 0.622)
c_{v1}	constant (= 7.1)
c_{w2}	constant (= 0.3)
c_{w3}	constant (= 2)
b_v	width of stem (m)
C_D	drag coefficient (−)
d	length scale
E	flexural stiffness (N/m^2),
F_i	(= F_x, F_y, F_z) are the resistance force components (N/m^3)
f_{rk}	vegetative resistance parameter (m^{-1})
f_v	vegetative resistance parameter (−)
h	water depth (m)
I	second moment of area (m^4)
k	turbulent kinetic energy (m^2 s^{-2})
k_d	deflection vegetation height (m)
k_v	vegetation height (m)
L	turbulent length scale (m)
M	bending moment (Nm)
n	vegetative Manning's roughness coefficient ($m^{-1/3}s$)
N	vegetation density (number of stems per m^2)
u_i	(= u, v, w) are the time-averaged velocity components (ms^{-1})
x_i	(= x, y, z) are the spatial coordinates (m)
z_0	zero plane displacement parameter (m)
Z'_o	modified zero plane displacement parameter (m)

Greek symbols

δ	deflection in x-direction (m)
α	constant (= *0.5*)
β	constant (= 0.7)
ζ	vegetation parameter (−)
ρ	water density (kg/m^3)
τ_{ij}	Reynolds stresses (N/m^2)
ν	new eddy viscosity variable (m^2 s^{-1})
ν_m	molecular viscosity (m^2 s^{-1})
ν_t	eddy viscosity (m^2 s^{-1})
κ	von Karman constant (−)
λ	scaling parameter (−)
ϖ	scaling parameter (> *0*)
α_o	scaling parameter (*between 0 and 1*)
β_o	scaling parameter (= 2)
σ	constant (= 2/3)

References

Baptist, M.J., Babovic, V., Keijzer, M., Uttenbogaard, R.E., Mynett, A., Verwey, A., 2007. On inducing equations for vegetation resistance. J. Hydraulic Res. 45 (4), 435–450.

Boller, M.L., Carrington, E., 2006. The hydrodynamic effects of shape and size during reconfiguration of a flexible macroalga. J. Exp. Biol. 209, 1894−1903.

Bowmer, K.H., Jacobs, S.W.L., Sainty, G.R., 1995. Indentification, biology and management of elodea canadensis, hydrocharitaceae. J. Aquatic Manag. 33, 13−19.

Brian, M.S., Shen, H.T., 2002. Hydraulic resistance of flow in channels with cylindrical roughness. J. Hydraulic Eng. 128 (5), 500−506.

Busari, A.O., Li, C.W., 2013. A hydraulic roughness model for submerged flexible vegetation. In: Proc. 2013 IAHR Congress, Beijing.

Carollo, F.G., Ferro, V., Termini, D., 2002. Flow measurement in vegetated channels. J. Hydraulic Eng. 128 (7), 664−673.

Carollo, F.G., Ferro, V., Termini, D., 2005. Flow resistance law in channels with flexible submerged vegetation. J. Hydraulic Eng. 131 (7), 554−564.

Cheng, N.S., 2011. Representative roughness height of submerged vegetation. J. Water Resour. Res. 47, 1−18.

Dunn, C., Lopez, F., Garcia, M., 1996. Mean Flow and Turbulence in a Laboratory Channel with Simulated Vegetation. In: Civil Engineering Studies. Hydraulic Engineering Series No.51.

Hofstra, D.E., Gemmill, C.E.C., Winton, M.D., 2006. Preliminary Genetic Assessment of New Zealand Isoetes and Nitella, Using DNA Sequencing and RAPDs, vol. 266. Science for Conservation.

Huai, W., Chen, Z., Han, J., 2009. Mathematical model for the flow with submerged and emerged rigid vegetation. J. Hydrodynamics 21 (5), 722−729.

Ikeda, S., Kanazawa, M., 1996. Three dimensional organized vortices above flexible water plants. J. Hydraulic Eng. 122 (11), 634−640.

Jarvela, J., 2005. Effect of submerged flexible vegetation on flow structure and resistance. J. Hydrology 307, 233−241.

Julier, S.J., 2002. The scaled unscented transformation. In: Proceedings of the American Control Conference, Anchorage, vol. 6, pp. 4555−4559.

Kevin, C., Johlene, K., Paul, C., 2007. Regional Guidelines for Ecological Assessments of Freshwater Environments: Aquatic Plants Cover in Wadeable Streams. Environment Waikato Technical report 2006/47.

Kim, K., Park, C.G., 2010. Non-symmetric unscented transformation with application to in- flight alignment. Int. J. Control, Automation, Syst. 8 (4), 776−781.

Klopstra, D., Barneveld, H.J., Noortwijk, J.M., Velzen, E.H., 1997. Analytical model for hydraulic roughness of submerged vegetation. In: The 27th Congress of IAHR, San Francisco, pp. 775−780.

Kouwen, N., Unny, T.E., 1973. Flexible roughness in open channels. J. Hydraulic Div. ASCE 99 (5), 713−728.

Li, C.W., Xie, J.F., 2011. Numerical modeling of free surface flow over submerged and highly flexible vegetation. Adv. Water Resour. 34, 468−477.

Li, C.W., Zeng, C., 2009. 3D numerical modeling of flow divisions at open channel junctions with or without vegetation. Adv. Water Resour. 32, 46−60.

Lopez, F., Garcia, M.H., 2001. Mean flow turbulence structure of open-channel flow through non- emergent vegetation. J. Hydraulic Eng. 127 (5), 392−402.

Meijer, D.G., 1998. Modelproeven Overstoomd Riet. Technical report PR177. HKV Consultants, Lelystad, The Netherlands.

Menezes, L.R., Soares, A.J.M., Silva, L.M., Ishihara, J.Y., 2013. Using unscented transform as alternative to Monte Carlo in bit error rate calculations. Electron. Lett. 2013 49 (10), 675−677.

Nikora, V., Scott, L., Nina, N., Koustuv, D., Glenn, C., Michael, R., 2008. Hydraulic resistance due to aquatic vegetation in small streams: field study. J. Hydraulic Eng. 134 (9), 1326−1332.

Poggi, D., Porporato, A., Ridolfi, L., Albertson, J.D., Katul, G.G., 2004. The effect of vegetation density on canopy sub-layer turbulence. Boundary-Layer Meteorol. 111, 565−587.

Raupach, M.R., 1994. Simplified expression for vegetation roughness length and zero-plane displacement as functions of canopy height and area index. Bound. Layer. Meteorol. 7, 211−216.

Spalart, P.R., Allmaras, S.R., 1994. A one-equation turbulence model for aerodynamic flows. La Rech. Aerosp. 1 (1), 5−21.

Stephan, U., Gutknecht, D., 2002. Hydraulic resistance of submerged flexible vegetation. J. Hydrology 269, 27−43.

Stéphanie, M., Hervé, D., Maxime, S., Nicholas, A., 2013. Fast parameter calibration of a cardiac electromechanical model from medical images based on the unscented transform. Biomech. Model Mechanobiol. 12, 815−831.

Taka-aki, O., Nezu, I., 2010. Flow resistance law in open-channel flows with rigid and flexible vegetation. River Flow. 2010.

Van der Merwe, R., 2004. Sigma-Point Kalman Filters for Probabilistic Inference in Dynamic State-space Models. Doctoral thesis. Oregon Health & Science University, United State.

Velasco, D., Bateman, A., Medina, V., 2008. A new integrated, hydro-mechanical model applied to flexible vegetation riverbeds. J. Hydraulic Res. 46 (5), 579−597.

Wilson, C.A.M.E., 2007. Flow resistance models for flexible submerged vegetation. J. Hydrology 342, 213−222.

Yang, W., Choi, S.U., 2010. A two-layer approach for depth-limited open-channel flows with submerged vegetation. J. Hydraulic Res. 48 (4), 466−475.

Zeng, C., 2011. Numerical and Experimental Studies of Flows in Open Channels with Gravel and Vegetation Roughnesses. PhD thesis. Department of Civil and Structural Engineering, The Hong Kong Polytechnic University, p. 197.